Inorganic Nanosystems for Therapeutic Delivery: Status and Prospects

Chang Soo Kim, **Gülen Yesilbag Tonga**, **David Solfiell**, and **Vincent M. Rotello**[*]
Department of Chemistry, University of Massachusetts, 710 North Pleasant Street, Amherst, MA, 01003, USA

Abstract

Inorganic nanomaterials have an array of structural and physical properties that can be used in therapeutic delivery systems. The sizes, shapes, and surfaces of inorganic nanomaterials can be tailored to produce distinct interactions with biological systems both *in vitro* and *in vivo*. Nanoparticle cores can likewise be engineered to possess unique opticophysical properties, including upconversion, size-dependent absorbance/emission as well as magnetic properties such as superparamagnetism. These properties make inorganic nanomaterials useful imaging agents for noninvasive diagnostics and remotely activated theragnostics. Taken together, these unique properties of inorganic nanomaterials make them promising delivery systems.

Keywords

inorganic nanomaterials; drug delivery; upconversion; theragnostic; multifunctional; imaging agent

1. Introduction

Inorganic nanomaterials are rapidly emerging tools for therapeutic delivery [1]. On the physical side, nanoparticle (NP) cores can be designed to retain unique optical properties that enable remote activation and imaging for theragnostic applications [2]. The cores of these materials also provide scaffolds featuring structural and dynamic properties difficult or impossible to access using other materials such as polymer and lipid-based delivery vectors. Taken together, these properties enable new strategies for the presentation and encapsulation of drugs, biomolecules, and imaging agents (Fig. 1).

In this highlight, we discuss selected recent advances in engineered inorganic nanosystems for delivery, diagnostic and theragnostic applications. We have divided this review into three categories: optical and magnetic properties of inorganic nanomaterials, the interaction of inorganic nanomaterials with their environment and applications of inorganic nanomaterials in imaging, delivery and theragnostics [3,4].

[*]Corresponding author. Prof. Vincent M. Rotello, Tel.: +1 413 545 2058; fax: +1 413 545 4490., rotello@chem.umass.edu.

2. Quantum properties of inorganic nanomaterials

Quantum confinement of excitons within nanoscale inorganic crystals is one of the unique properties that distinguishes nanomaterials from their corresponding bulk solids [5]. Some of the benefits of quantum dots (QDs) with respect to fluorescent organic dyes are broad absorption spectra with narrow, size-tunable emissions that possess superior signal brightness and greater resistance to photobleaching. QDs can be functionalized with synthetic ligands that simultaneously passivate the inorganic core and provide the particles with additional functionalities. Together, these properties make QDs versatile nanoscale scaffolds for designing multifunctional NPs with both imaging and therapeutic functions [6].

Beside quantum confinement, another noteworthy feature of inorganic materials is capacity for the upconversion (UC) of light energy. In upconversion, the particle emits higher energy photons after being excited by multiple lower-energy photons (usually near-infrared (NIR) or infrared IR radiation) [7]. Upconverting particles are typically designed to emit visible light upon NIR-light excitation. NIR-to-Vis UC imaging systems allow the light source to penetrate more deeply into living tissues than down-conversion luminescent materials that often suffer from low signal-to-noise ratios as a result of shallow tissue-penetration depth (Fig. 2) [8,9]. Recently, Li et al. have reported the first example of triplet-triplet annihilation (TTA)-based UC system used for *in vivo* whole-body imaging [8]. Both sensitizer (octaethylporphyrin Pd complex) and annihilator (9,10-diphenylanthracene) have been successfully embedded into a silica NP to obtain a water-soluble TTA-based UC NP. These NPs demonstrate low cytotoxicity and high photo-stability, and exhibit quantum yields of 4.5 % in pure water.

3. The interface between nanoparticles and biosystems

Many factors affect the interactions between NPs and biological systems. The interfacial forces between NPs and biological membranes can be expressed mathematically in terms of particle 'wrapping time'. Wrapping time is related to particle size and shape, as well as membrane surface energy and elasticity [10]. Chan et al. have observed differences in cellular uptake in a number of cell lines (A549, HeLa and MDA-MB 435) as a function of several physical aspects of NPs, including size and shape [11, 12]. This same group has described a protein 'corona' effect in which NPs become surrounded by a protein coat after being exposed to serum or extracellular environments. Biological coatings of this kind mask the synthetic identity of nanomaterials and provide them with biological properties. Xia et al. have also investigated the dependence of physical parameters (size, shape, density and surface coating) on the cellular uptake of inorganic NPs employing an inverted cell culture system to minimize sedimentation effects [13]. Size-dependent distribution of water-soluble QDs *in vivo* has been investigated in real time by the simultaneous injection and imaging of QDs (Fig. 3) [14]. Multiphoton microscopy images demonstrate that QDs (< 60 nm) are able to extravasate and diffuse away from blood vessels while 125 nm QDs do not extravasate due to interstitial transport barriers (Fig. 3 b-c).

The interaction between inorganic nanomaterials and biological systems is also strongly affected by surface chemistry with Rotello et al. observing strong interactions of cationic NPs with cells [15, 16].

4. Applications for inorganic nanomaterials

4.1. Imaging applications of inorganic nanomaterials

Noninvasive imaging technologies, such as magnetic resonance imaging (MRI), optical imaging, positron emission tomography (PET), computed X-ray tomography, photothermal

heterodyne imaging and ultrasound, play a critical role in clinical diagnoses and treatment [17, 18]. Inorganic NPs provide multifunctional agents for noninvasive imaging applications as a result of their magnetic and optical properties. These optical properties can be tuned by controlling the assembly process of inorganic nanomaterials via programmable intermolecular interactions [19]. Superparamagnetic iron oxides (SPIO) NPs may be used as MRI contrast agents, and have been used to image a number of organs in mice, including bowel, liver, and spleen [20]. Improved contrast in cancer imaging has been achieved using surface functionalized inorganic NPs carrying tumor-specific targeting ligands [21]. Inorganic NP imaging agents can assist cancer treatments by providing surgeons with the means of identifying tumor margins for resection procedures [22].

Gold NPs (AuNPs) provide promising optical contrast agents as a result of their size and shape dependent optical properties as well as their general biocompatibility. Nanospheres, nanocages, nanorods and nanoshells made from AuNPs have all been used as contrast agents in preclinical investigations [21]. NP imaging agents can compliment traditional imaging methods when used in multimodal imaging strategies. For example, the shallow tissue penetration of photoacoustic imaging with NPs can be complimented by the low-resolution deep tissue imaging of ultrasound [23, 24]. In Fig 4., photoacoustic images (Fig. 4 b-f) were used to identify one of four cell groups from the ultrasound image (Fig. 4a) that have been labeled with targeted AuNPs [24]. Together, the two imaging modalities produce a highly informative image of the diseased site. Furthermore, multimodal imaging can be used to map the distribution and clearance of NPs. Prasad et al. synthesized organically modified silica NPs conjugated with near-infrared fluorophores for optical imaging with maximum tissue penetration [25]. In addition, the NPs were radiolabeled with ^{124}I for PET imaging making accurate NP quantification within various target organs possible after injection in mice. Biodistribution results show accumulation of NPs in the major reticuloendothelial system organs (e.g., liver, spleen and stomach), and a clearance study indicates hepatobiliary excretion of NPs.

4.2. Application of inorganic nanomaterials in drug delivery

Nanomaterial-based drug delivery systems are highly attractive platforms for the efficient delivery and release of drugs to targeted tissues and cells. There are two major strategies for conjugating drugs to NPs: covalent or non-covalent association [26, 27]. Mirkin et al. have employed a covalent attachment strategy to conjugate paclitaxel (a potent chemotherapeutic drug) to AuNPs via DNA linkers, thereby enhancing the solubility and overall effectiveness of the drug [28]. Also, Zubarev et al. have attached a flexible hexaethylene glycol linker to the C-7 position of paclitaxel to conjugate it to phenol-terminated Au NPs [29]. Using this strategy, 70 molecules of paclitaxel were able to be loaded onto an AuNP in a controlled manner.

Rotello et al. have used the hydrophobic interior of Au NP monolayers to non-covalently encapsulate and deliver a hydrophobic drug molecule [30]. Depending on the strategy used, the release of a drug from its carrier can be triggered by a wide range of stimuli, such as hydrophobicity, pH, temperature, magnetic fields, enzymes, UV, and NIR photoluminescence [30, 31, 32, 33, 34, 35]. For instance, Burda et al. have shown a photodynamic therapy (PDT) drug such as silicon phthalocyanine 4 could be successfully adsorbed on PEGylated AuNPs and used as an effective PDT drug delivery vector for both *in vitro* and *in vivo* applications [36]. Also, Sun et al. have reported that a hydrophobic drug (cisplatin) can be loaded and released in low pH (<6) using porous hollow Fe_3O_4 NPs [37].

Inorganic nanomaterials can be designed to improve drug efficacy through enhanced targeting delivery [38]. For instance, El-Sayed et al. have quantified the degree of tumor cell uptake of Au nanorods covalently conjugated to tumor-targeting peptides [39]. Cheon et al.

have created a multifunctional "all-in-one" magnetic NP comprising a cell-specific targeting moiety, a fluorescent dye, and a therapeutic siRNA payload to target images, and diseased cells simultaneously [40].

Inorganic nanomaterials can also be used as therapeutic agents themselves. Rotello et al. have reported the use of synthetic host–guest chemistry involving diaminohexane-terminated AuNPs (AuNP–NH$_2$) and complementary cucurbit[7]uril (CB[7]) to provide a triggered activation of a therapeutic system (Fig. 5) [41]. Cytotoxicity in this system is triggered by removal of CB[7] in the presence of 1-adamantylamine.

4.3. Theragnostic applications of inorganic nanomaterials

The combination of imaging and therapeutic systems generates a hybrid delivery platform, called "theragnostics". The inherent properties of inorganic NPs, such as a facile surface modification, high surface to volume ratios, controllable shape/size, and unique optical properties, make them excellent candidates for theragnostic applications [42]. El-Sayed et al. have designed multifunctional anti-cancer AuNPs that can act as targeted contrast agents for photothermal cancer therapy and as scaffolds for enhanced potent cancer drug delivery [43].

The ability to functionalize magnetic NPs with targeting, therapeutic, and imaging moieties makes magnetic NPs an ideal platform for theragnostics [44]. Additionally, the thermal energy from magnetic NPs can be used as an external and a remotely regulated trigger for controlled drug release. Zink et al. have described a novel material that incorporates zinc-doped iron oxide nanocrystals within a pseudorotaxane functionalized mesoporous silica framework for the delivery of the cargo, with release effected by magnetic heating [45]. Zhang et al. have reported the facile synthesis of a hydrophilic multifunctional dual imaging mode mesoporous nanorattles making use of both its UC luminescent and magnetic properties [46]. Upon application of an alternating magnetic field, the thermal energy generated by the magnetic particles releases the drug by opening the gates of mesoporous silica carriers (Fig. 6). The concept of theragnostic dual imaging NPs with external stimuli can be applied in many biomedical applications by engineering additional functionalities onto the NPs.

5. Conclusions

The unique physical and chemical properties of inorganic nanomaterials contribute to their wide range of possible applications in imaging, drug delivery, and theragnostics. Quantum confinement, facile size/shape and surface modification, and tunable optical properties make inorganic nanoparticles versatile design platforms for multifunctional biomedical technologies. Taken together, inorganic particles provide excellent tools for fundamental research and candidates for therapeutic, imaging, and theragnostic applications.

Acknowledgments

References

1. Petros RA, DeSimone JM. Strategies in the design of nanoparticles for therapeutic applications. Nat. Rev. Drug Discov. 2010; 9:615–627. [PubMed: 20616808]

2. Jokerst JV, Gambhir SS. Molecular imaging with theranostic nanoparticles. Acc. Chem. Res. 2011; 44:1050–1060. [PubMed: 21919457]

3. Kumar CS, Mohammad F. Magnetic nanomaterials for hyperthermia-based therapy and controlled drug delivery. Adv. Drug Deliv. Rev. 2011; 63:789–808. [PubMed: 21447363]

4. Doane TL, Burda C. The unique role of nanoparticles in nanomedicine: imaging, drug delivery and therapy. Chem. Soc. Rev. 2012; 41:2885–2911. [PubMed: 22286540]

5. Irrera A, Artoni P, Iacona F, Pecora EF, Franzo G, Galli M, Fazio B, Boninelli S, Priolo F. Quantum confinement and electroluminescence in ultrathin silicon nanowires fabricated by a maskless etching technique. Nanotechnology. 2012; 23:075204. [PubMed: 22273546]

6. Smith AM, Duan H, Mohs AM, Nie S. Bioconjugated quantum dots for *in vivo* molecular and cellular imaging. Adv. Drug Deliv. Rev. 2008; 60:1226–1240. [PubMed: 18495291]

7. Chatterjee DK, Gnanasammandhan MK, Zhang Y. Small upconverting fluorescent nanoparticles for biomedical applications. Small. 2010; 6:2781–2795. [PubMed: 21064086]

8. Liu Q, Yang T, Feng W, Li F. Blue-emissive upconversion nanoparticles for low-power-excited bioimaging *in vivo*. J. Am. Chem. Soc. 2012; 134:5390–5397. [PubMed: 22369318]

9. Li Z, Zhang Y, Jiang S. Multicolor core/shell-structured upconversion fluorescent nanoparticles. Adv. Mater. 2008; 20:4765–4769.

10. Nel AE, Madler L, Velegol D, Xia T, Hoek EMV, Somasundaran P, Klaessig F, Castranova V, Thompson M. Understanding biophysicochemical interactions at the nano-bio interface. Nat. Mater. 2009; 8:543–557. [PubMed: 19525947]

11. Walkey CD, Chan WC. Understanding and controlling the interaction of nanomaterials with proteins in a physiological environment. Chem. Soc. Rev. 2012; 41:2780–2799. [PubMed: 22086677]

12. Albanese A, Chan WCW. Effect of gold nanoparticle aggregation on cell uptake and toxicity. ACS Nano. 2011; 5:5478–5489. [PubMed: 21692495]

13. Cho EC, Zhang Q, Xia YN. The effect of sedimentation and diffusion on cellular uptake of gold nanoparticles. Nat. Nanotechnol. 2011; 6:385–391. [PubMed: 21516092]

14. Popovic Z, Liu W, Chauhan VP, Lee J, Wong C, Greytak AB, Insin N, Nocera DG, Fukumura D, Jain RK, Bawendi MG. A nanoparticle size series for *in vivo* fluorescence imaging. Angew. Chem. Int. Ed. Engl. 2010; 49:8649–8652. [PubMed: 20886481]

15. Zhu ZJ, Ghosh PS, Miranda OR, Vachet RW, Rotello VM. Multiplexed screening of cellular uptake of gold nanoparticles using laser desorption/ionization mass spectrometry. J. Am. Chem. Soc. 2008; 130:14139–14143. [PubMed: 18826222]

16. Goodman CM, McCusker DC, Yilmaz T, Rotello VM. Toxicity of gold nanoparticles functionalized with cationic and anionic sidechains. Bionconj. Chem. 2004; 15:897–900.

17. Na HB, Song IC, Hyeon T. Inorganic nanoparticles for MRI contrast agents. Adv. Mater. 2009; 21:2133–2148.

18. Leduc C, Jung J-M, Carney RR, Stellacci F, Lounis B. Direct investigation of intracellular presence of gold nanoparticles *via* photothermal heterodyne imaging. ACS Nano. 2011; 5:2587–2592. [PubMed: 21388224]

19. Aili D, Gryko P, Sepulveda B, Dick JAG, Kirby N, Heenan R, Baltzer L, Liedberg B, Ryan MP, Stevens MM. Polypeptide folding-mediated tuning of the optical and structural properties of gold nanoparticle assemblies. Nano Lett. 2011; 11:5564–5573. [PubMed: 22047629]

20. Sun C, Lee JS, Zhang M. Magnetic nanoparticles in MR imaging and drug delivery. Adv. Drug Deliv. Rev. 2008; 60:1252–1265. [PubMed: 18558452]

21. Cho EC, Glaus C, Chen JY, Welch MJ, Xia YN. Inorganic nanoparticle-based contrast agents for molecular imaging. Trends Mol. Med. 2010; 16:561–573. [PubMed: 21074494]

22. Sullivan DC, Ferrari M. Nanotechnology and tumor imaging: seizing an opportunity. Mol. Imaging. 2004; 3:364–369. [PubMed: 15802054]

23. Gary-Bobo M, Hocine O, Brevet D, Maynadier M, Raehm L, Richeter S, Charasson V, Loock B, Morere A, Maillard P, Garcia M, Durand JO. Cancer therapy improvement with mesoporous silica nanoparticles combining targeting, drug delivery and PDT. Int. J. Pharm. 2012; 423:509–515. [PubMed: 22178618]

24. Mallidi S, Larson T, Tam J, Joshi PP, Karpiouk A, Sokolov K, Emelianov S. Multiwavelength photoacoustic imaging and plasmon resonance coupling of gold nanoparticles for selective detection of cancer. Nano Lett. 2009; 9:2825–2831. [PubMed: 19572747]

25. Kumar R, Roy I, Ohulchanskky TY, Vathy LA, Bergey EJ, Sajjad M, Prasad PN. In vivo biodistribution and clearance studies using multimodal organically modified silica nanoparticles. ACS Nano. 2010; 4:699–708. [PubMed: 20088598]

26. Anglin EJ, Cheng L, Freeman WR, Sailor MJ. Porous silicon in drug delivery devices and materials. Adv. Drug Deliv. Rev. 2008; 60:1266–1277. [PubMed: 18508154]

27. Bhattacharyya S, Kudgus RA, Bhattacharya R, Mukherjee P. Inorganic nanoparticles in cancer therapy. Pharm. Res. 2011; 28:237–259. [PubMed: 21104301]

28. Zhang X-Q, Xu X, Lam R, Giljohann D, Ho D, Mirkin CA. Solubility and efficacy through covalent attachment to polyvalent DNA-nanoparticle conjugates. ACS Nano. 2011; 5:6962–6970. [PubMed: 21812457]

29. Gibson JD, Khanal BP, Zubarev ER. Paclitaxel-functionalized gold nanoparticles. J. Am. Chem. Soc. 2007; 129:11653–11661. [PubMed: 17718495]

30. Kim CK, Ghosh P, Pagliuca C, Zhu ZJ, Menichetti S, Rotello VM. Entrapment of hydrophobic drugs in nanoparticle monolayers with efficient release into cancer cells. J. Am. Chem. Soc. 2009; 131:1360–1361. [PubMed: 19133720]

31. Timko BP, Dvir T, Kohane DS. Remotely triggerable drug delivery systems. Adv. Mater. 2010; 22:4925–4943. [PubMed: 20818618]

32. de la Rica R, Aili D, Stevens MM. Enzyme-responsive nanoparticles for drug release and diagnostics. Adv. Drug Deliv. Rev. 2012; 64:967–978. [PubMed: 22266127]

33. Agasti SS, Chompoosor A, You CC, Ghosh P, Kim CK, Rotello VM. Photoregulated release of caged anticancer drugs from gold nanoparticles. J. Am. Chem. Soc. 2009; 131:5728–5729. [PubMed: 19351115]

34. Park JH, Gu L, von Maltzahn G, Ruoslahti E, Bhatia SN, Sailor MJ. Biodegradable luminescent porous silicon nanoparticles for *in vivo* applications. Nat. Mater. 2009; 8:331–336. [PubMed: 19234444]

35. Park JH, von Maltzahn G, Ong LL, Centrone A, Hatton TA, Ruoslahti E, Bhatia SN, Sailor MJ. Cooperative nanoparticles for tumor detection and photothermally triggered drug delivery. Adv. Mater. 2010; 22:880–885. [PubMed: 20217810]

36. Cheng Y, Samia AC, Meyers JD, Panagopoulos I, Fei B, Burda C. Highly efficient drug delivery with gold nanoparticle vectors for in vivo photodynamic therapy of cancer. J. Am. Chem. Soc. 2008; 130:10643–10647. [PubMed: 18642918]

37. Cheng K, Peng S, Xu C, Sun S. Porous hollow Fe(3)O(4) nanoparticles for targeted delivery and controlled release of cisplatin. J. Am. Chem. Soc. 2009; 131:10637–10644. [PubMed: 19722635]

38. Cheng Y, Meyers JD, Agnes RS, Doane TL, Kenney ME, Broome A-M, Burda C, Basilion JP. Addressing brain tumors with targeted gold nanoparticles: A new gold standard for hydrophobic drug delivery? Small. 2011; 7:2301–2306.

39. Huang X, Peng X, Wang Y, Wang Y, Shin DM, El-Sayed MA, Nie S. A Reexamination of active and passive tumor targeting by using rod-shaped gold nanocrystals and covalently conjugated peptide ligands. ACS Nano. 2010; 4:5887–5896. [PubMed: 20863096]

40. Lee JH, Lee K, Moon SH, Lee Y, Park TG, Cheon J. All-in-one target-cell-specific magnetic nanoparticles for simultaneous molecular imaging and siRNA delivery. Angew. Chem. Int. Ed. Engl. 2009; 48:4174–4179. [PubMed: 19408274]

41. Kim C, Agasti SS, Zhu ZJ, Isaacs L, Rotello VM. Recognition-mediated activation of therapeutic gold nanoparticles inside living cells. Nat. Chem. 2010; 2:962–966. [PubMed: 20966953]

42. Xie J, Lee S, Chen X. Nanoparticle-based theranostic agents. Adv. Drug Deliv. Rev. 2010; 62:1064–1079. [PubMed: 20691229]

43. Dreaden EC, Mackey MA, Huang XH, Kang B, El-Sayed MA. Beating cancer in multiple ways using nanogold. Chem. Soc. Rev. 2011; 40:3391–3404. [PubMed: 21629885]

44. Yoo D, Lee JH, Shin TH, Cheon J. Theranostic magnetic nanoparticles. Acc. Chem. Res. 2011; 44:863–874. [PubMed: 21823593]

45. Thomas CR, Ferris DP, Lee JH, Choi E, Cho MH, Kim ES, Stoddart JF, Shin JS, Cheon J, Zink JI. Noninvasive remote-controlled release of drug molecules *in vitro* using magnetic actuation of mechanized nanoparticles. J. Am. Chem. Soc. 2010; 132:10623–10625. [PubMed: 20681678]

46. Zhang F, Braun GB, Pallaoro A, Zhang Y, Shi Y, Cui D, Moskovits M, Zhao D, Stucky GD. Mesoporous multifunctional upconversion luminescent and magnetic "nanorattle" materials for targeted chemotherapy. Nano Lett. 2012; 12:61–67. [PubMed: 22133237]
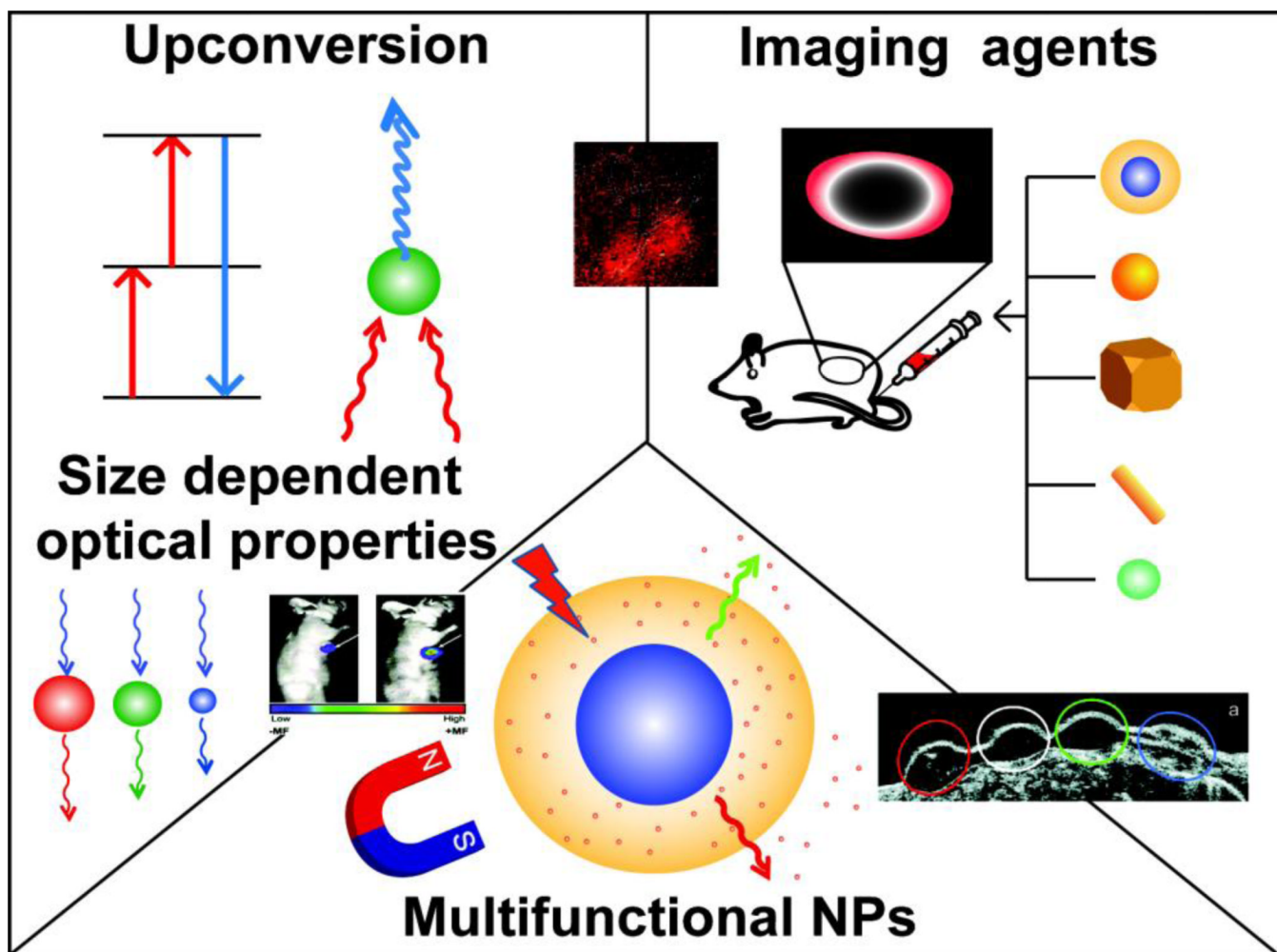
Fig. 1.
Schematic presentation of inorganic nanomaterials with different sizes and shapes. The inorganic nanomaterials possess various physical, chemical properties and may be used in numerous applications in imaging, delivery, and theragnostic applications.
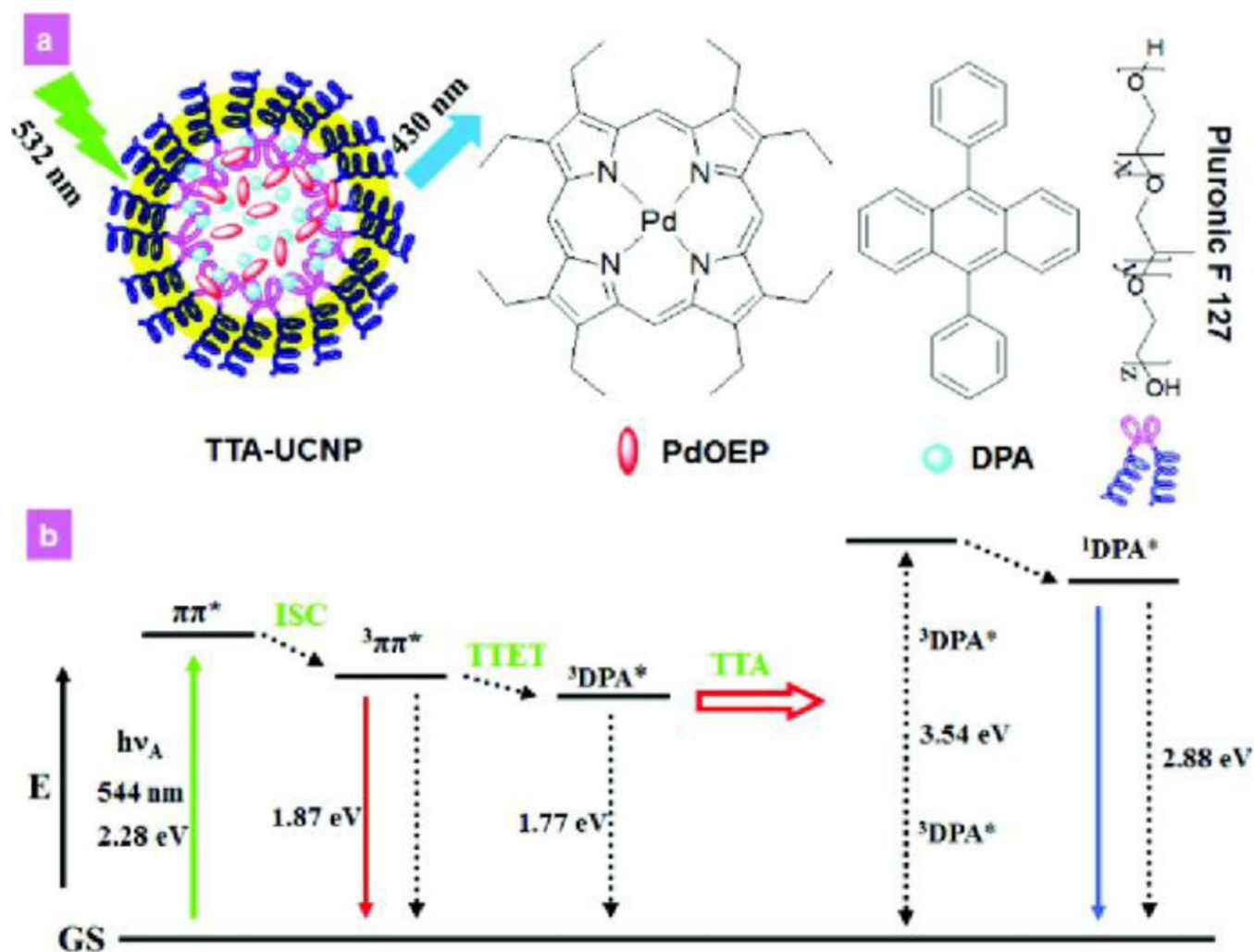
Fig. 2.
(a) Schematic illustration of upconversion luminescence of NPs triplet–triplet annihilation - upconversion nanophosphors NPs (TTA-UCNP), and chemical structures of building blocks for TTA-UCNP. (b) Energy level diagram of sensitized TTA process. (Reproduced with permission from [8], copyright by the American Chemical Society).
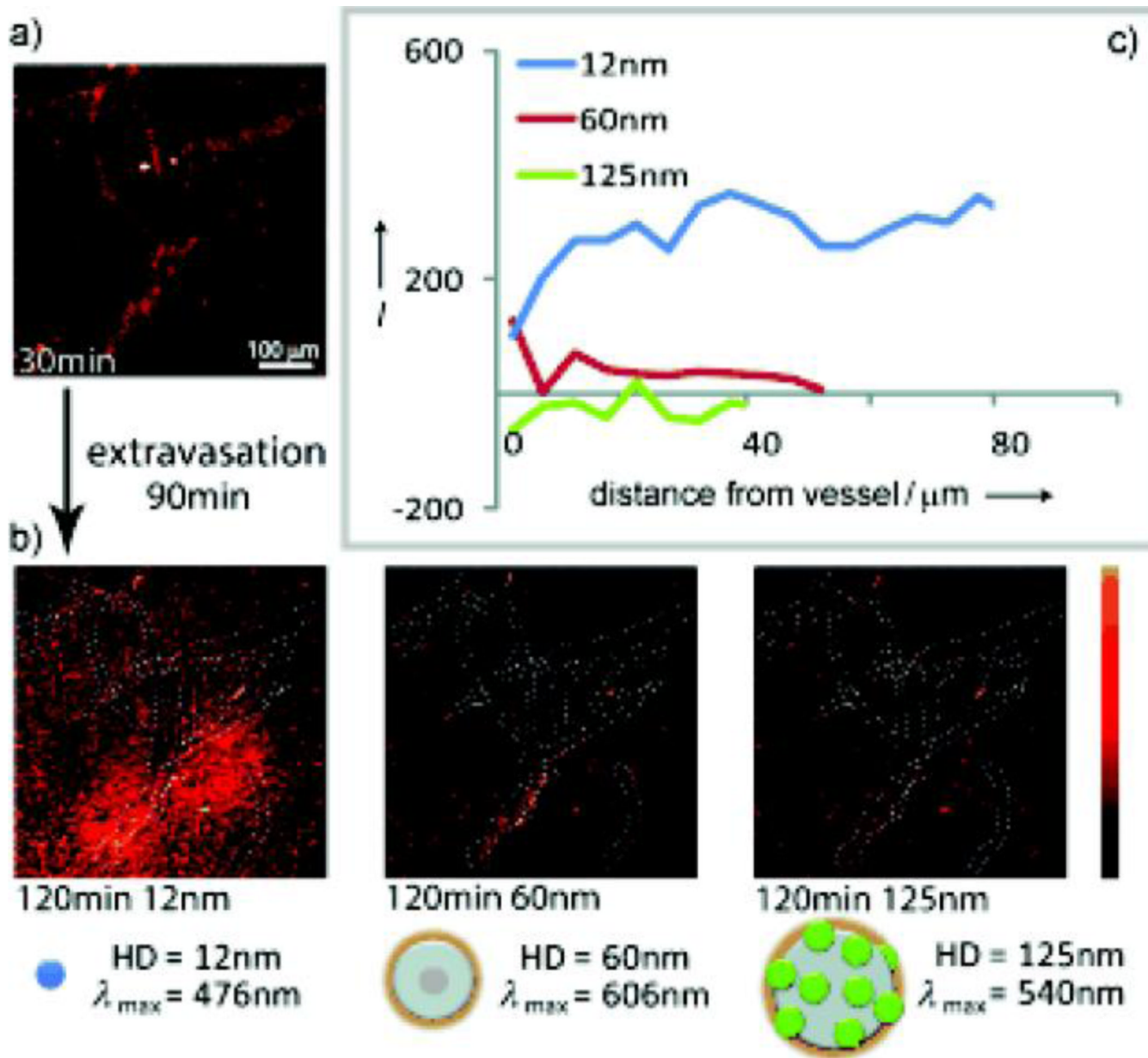
Fig. 3.
Real-time intravital imaging of size-dependent QDs distribution in a SCID mouse bearing a Mu89 melanoma. (a) Multiphoton microscopy image of the distribution of NPs at 30 min. (b) Multiphoton microscopy images of distribution of the NPs in the same region as (a) at 120 min post-injection. (c) Penetration depth analysis at 60 min post-injection. (Reproduced with permission from [14], copyright by the John Wiley and Sons)
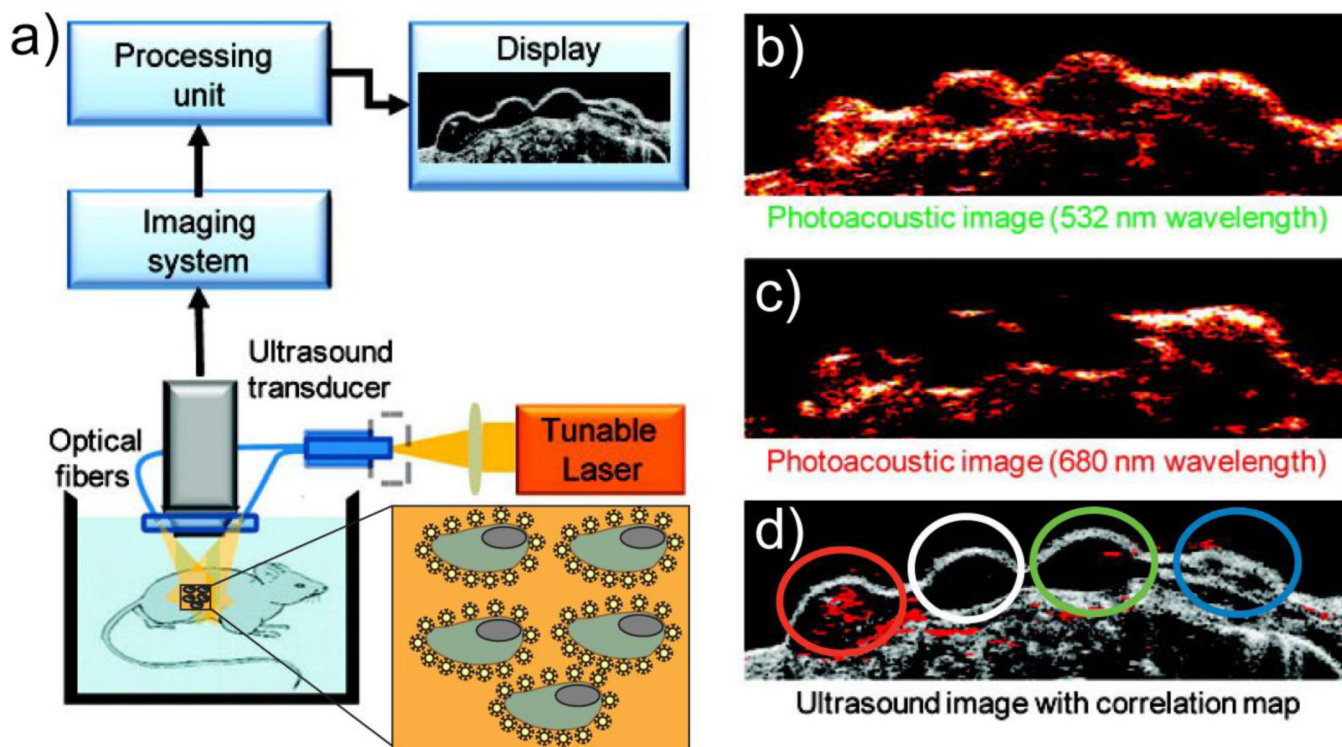
Fig. 4.
Block diagram of the combined ultrasound and photoacoustic imaging system (a), photoacoustic images (b,c) and ultrasound (d) of gelatin implants in mouse tissue *ex vivo* at various laser illumination wavelengths. The cells with targeted AuNPs (red), control cells (white), the cells mixed with mPEG-SH coated Au NPs (green), and NIR dye (blue) are shown on the ultrasound image (d). (Reproduced with permission from [24], copyright by the American Chemical Society)
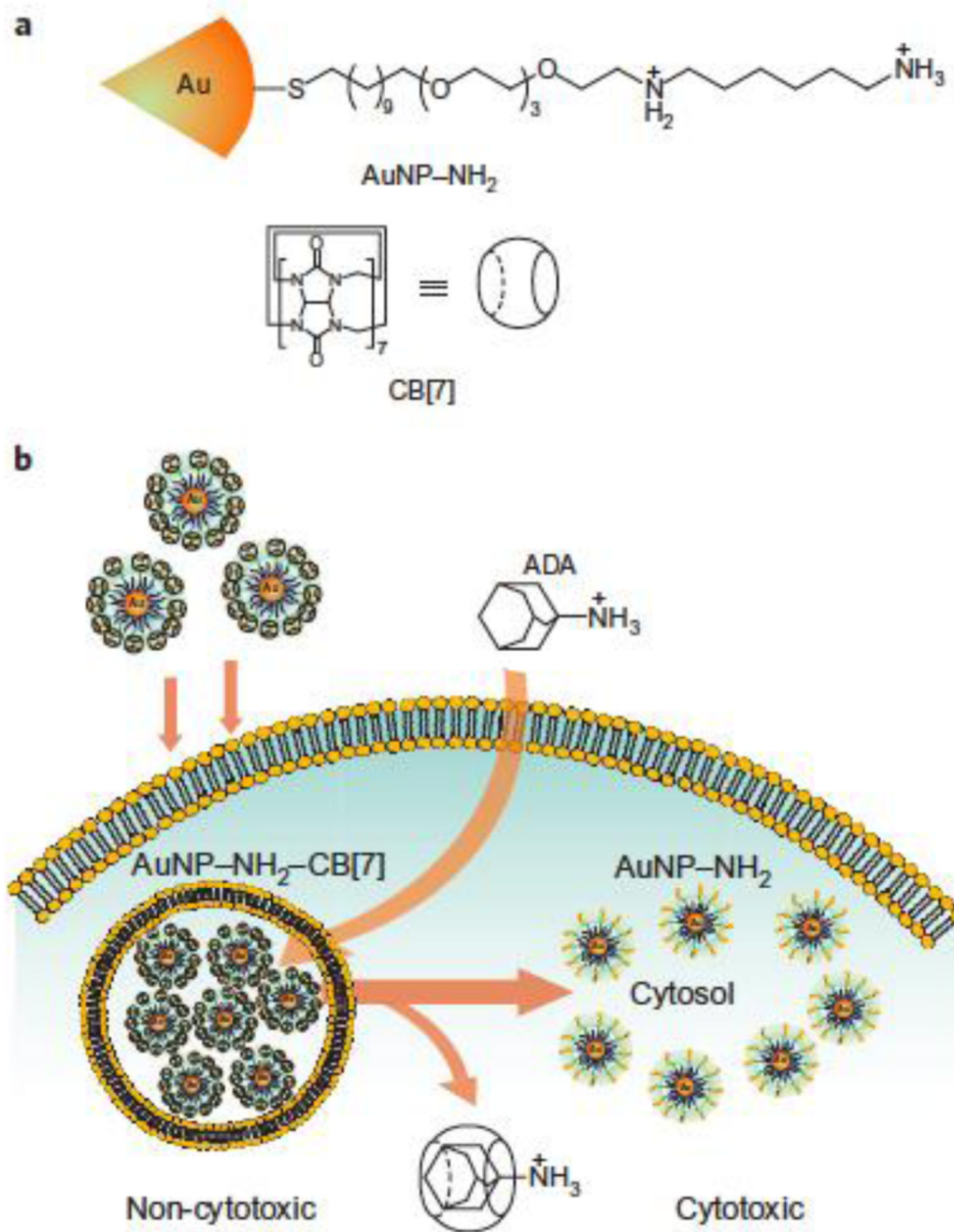
Fig. 5.
(a) Structure of the diaminohexane-terminated AuNP and cucurbit[7]uril (CB[7]). (b) Activation of AuNP–NH$_2$–CB[7] cytotoxicity by dethreading of CB[7] from the NP surface by 1-adamatylamine. (Reproduced with permission from [41], copyright by the Nature Publishing Group)
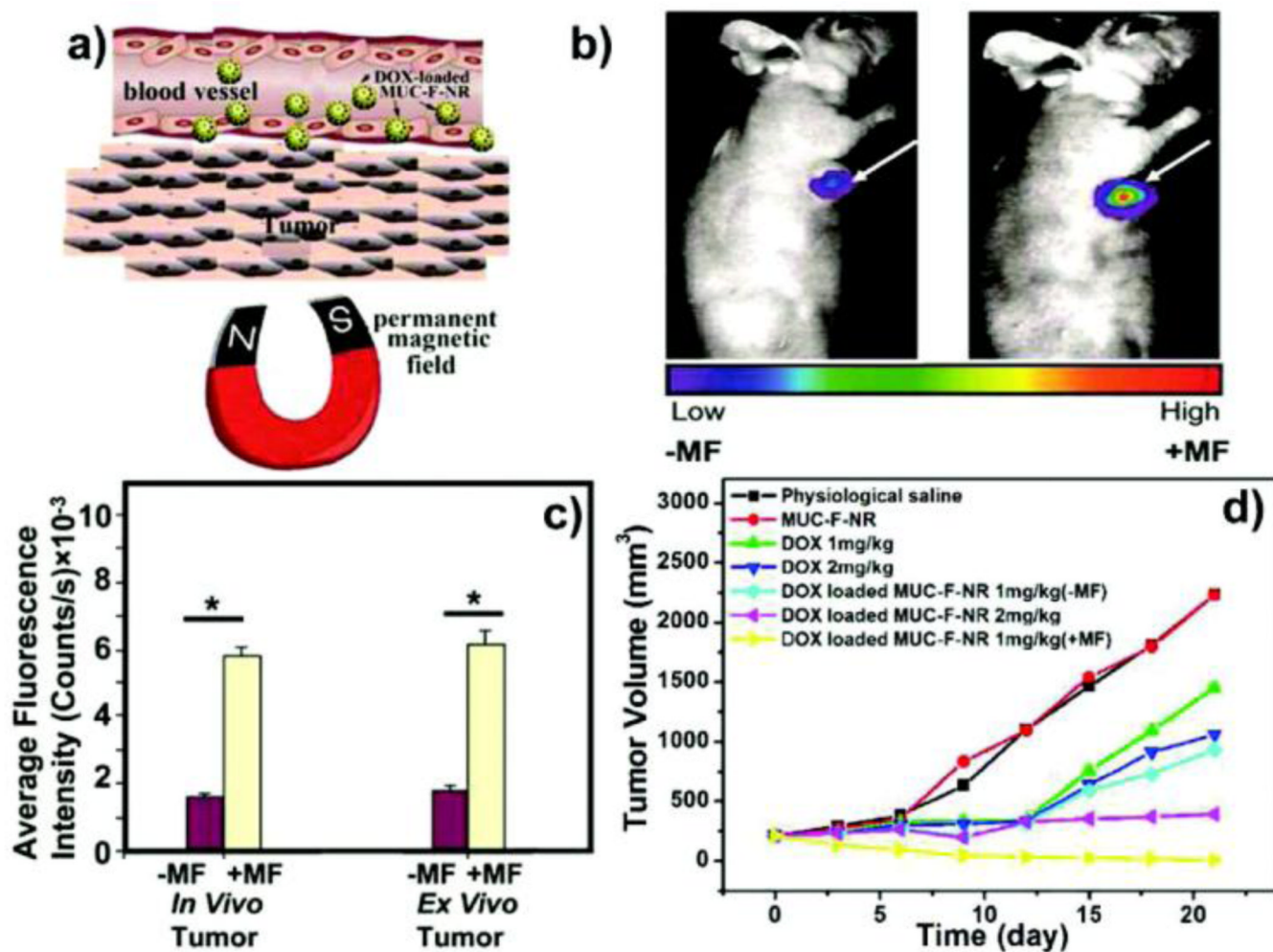
Fig. 6.
(a) Schematic presentation of targeting of doxorubicin (DOX) loaded magnetic upconversion oxide nanospheres (MUC-F-NR) to tumor cells assisted by an externally applied magnetic field (MF). (b) Tumor location intensity increases with 1 h magnetic field treatment. (c) The luminescence signal at 650 nm. (d) Changes in tumor volume of mice treated with saline, MUC-F-NR, DOX, and DOX loaded MUC-F-NR over 21 days in the absence and presence of MF. (Reproduced with permission from [46], copyright by the American Chemical Society)